

Excitation of *L*-Shell Electrons in Al and Al₂O₃ by 20-keV Electrons*

N. SWANSON AND C. J. POWELL

Institute for Basic Standards, National Bureau of Standards, Washington, D. C. 20234

(Received 5 July 1967)

The energy-loss distributions of ≈ 20 -keV electrons transmitted through 210–575 Å-thick specimens of Al and Al₂O₃ have been measured at zero scattering angle. Two types of Al₂O₃ were used: films of the γ phase and amorphous films prepared by anodization. Loss spectra were obtained for an energy-loss range of 0–160 eV, in which structure due to *L*-shell excitation in Al and Al₂O₃ was observed. The positions of the absorption edges and of the peaks on the high-energy-loss side of each edge agreed well with recent x-ray absorption measurements. Slightly different structure for the two forms of Al₂O₃ was found near the edge, as recently found by x-ray absorption. From the observed intensities, the values of oscillator strengths, mass-absorption coefficients, and electron-scattering cross sections have been derived for each material up to ≈ 85 eV beyond the absorption edge. The Al results are in good agreement with recent x-ray measurements and are consistent with the Al₂O₃ data. The similarity in the electron energy-loss and x-ray absorption measurements is consistent with the equality of the longitudinal and transverse dielectric constants $\epsilon(\omega)$ and with the expectation that in this energy-loss region $\text{Im}\epsilon = -\text{Im}1/\epsilon$ to a good approximation.

1. INTRODUCTION

THE excitation of valence electrons in solids by incident electrons of 100 eV–100 keV energy has been observed in many experiments, but relatively few measurements have been made of the excitation of inner-shell electrons. Ruthemann¹ observed energy losses corresponding to the excitation of *K*-shell electrons in C, N, and O when 7.5-keV electrons were transmitted through thin films of collodion. Hillier and Baker² similarly found energy-loss peaks due to *K*-shell excitation in Be, C, N, O, Al, and Si, to *L*-shell excitation in Fe and Zn, and to *M*-shell excitation in Fe using primary electrons of 26–65 keV energy. More recently, energy-loss peaks identified as being due to the excitation of outer core electrons have been observed in transmission experiments using ≈ 50 -keV electrons and in reflection experiments using ≈ 1 -keV electrons.^{3,4} Watanabe⁴ has observed the onset of excitation of *L*-shell electrons in both Al and Al₂O₃, together with structure which he has compared with that observed on the high-energy side of the Al x-ray absorption edge.⁵

The purpose of this paper is to report measurements of the excitation of *L*-shell electrons in Al and two forms of Al₂O₃. Energy-loss spectra have been obtained using ≈ 20 -keV primary electrons transmitted through thin specimen films. "Fine structure" observed for energy losses greater than the threshold excitation energy for each material has been compared with x-ray-absorption data. In addition, using a technique discussed in a

previous paper,⁶ it has been possible over the range of measurement to obtain oscillator strengths, x-ray-absorption coefficients, and an estimate of the total cross section for creation of the inner-shell vacancy by the primary electron.

2. THEORY

It can be shown⁷ that the doubly differential cross section per atomic electron for an excitation involving energy loss $E = \hbar\omega$ and momentum transfer q can be expressed in the form

$$\frac{d^2\sigma}{d\omega dq} = -\frac{2e^2}{\pi N \hbar v^2} \text{Im} \left[\frac{1}{\epsilon(\omega, q)} \right] \frac{1}{q}. \quad (1)$$

In this equation, N is the total electron density, v is the velocity of the primary electrons, and $\text{Im}[1/\epsilon(\omega, q)]$ is the imaginary part of the reciprocal complex dielectric constant $\epsilon = \epsilon_1 + i\epsilon_2$, a function of frequency ω and of q .

Following Fano,⁷ and Glick and Ferrell,⁷ Eq. (1) may be related to microscopic theories⁸ of inelastic scattering by defining a differential oscillator strength

$$\frac{df}{d\omega} = -\frac{\omega \text{Im}[1/\epsilon(\omega, q)]}{\frac{1}{2}\pi\Omega_p^2}, \quad (2)$$

where $\Omega_p = (4\pi N e^2/m)^{1/2}$. The Thomas-Reiche-Kuhn^{7,8} sum rule becomes

$$\int_0^\infty (df/d\omega) d\omega = 1, \quad (3a)$$

and

$$n_{\text{eff}}(E) = Z \int_0^E [df/d(\hbar\omega)] d(\hbar\omega) \quad (3b)$$

* Work supported partially by the Atomic Energy Commission, Division of Biology and Medicine.

¹ G. Ruthemann, *Naturwiss.* **30**, 145 (1942); *Ann. Physik* **6**, 135 (1948).

² J. Hillier and R. F. Baker, *J. Appl. Phys.* **15**, 663 (1944).

³ J. L. Robins and J. B. Swan, *Proc. Phys. Soc. (London)* **76**, 857 (1960); J. L. Robins, *ibid.* **79**, 119 (1962); P. E. Best, *ibid.* **80**, 1308 (1962); J. Geiger, P. Odolga, and H.-Chr. Pfeiffer, *Phys. Status Solid.* **15**, 531 (1966); M. Creuzburg, *Z. Physik* **196**, 433 (1966); A. V. Crewe, *Science* **154**, 729 (1966).

⁴ H. Watanabe, *J. Appl. Phys. Japan* **3**, 804 (1964).

⁵ D. H. Tomboulian and E. M. Pell, *Phys. Rev.* **83**, 1196 (1951).

⁶ N. Swanson and C. J. Powell, *Phys. Rev.* **145**, 195 (1966).

⁷ J. Hubbard, *Proc. Phys. Soc. (London)* **A68**, 976 (1955); U. Fano, *Phys. Rev.* **103**, 1202 (1956); A. J. Glick and R. A. Ferrell, *Ann. Phys. (N. Y.)* **11**, 359 (1960); D. Pines, in *Elementary Excitations in Solids* (W. A. Benjamin, Inc., New York, 1963).

⁸ H. Bethe, *Ann. Physik* **5**, 325 (1930).

represents the effective number of electrons per atom participating in the various excitation processes, up to energy loss E . Here Z must be regarded as the number of electrons per atom or unit molecule of the solid, since the sum rule applies to the whole atom or molecule under consideration.⁹ In this work, the lower limit of the integration is replaced by E_{nl} , the binding energy of electrons in the nl shell, so that Eq. (3b) can be used to derive the number of nl shell electrons per atom contributing to the absorption in a particular energy-loss range. Equation (1) can now be written

$$\frac{d^2\sigma}{d\omega dq} = \frac{4\pi e^4}{mv^2} \frac{1}{q} \frac{1}{E} \frac{df}{d\omega}. \quad (4)$$

The dependence of $df/d\omega$ on q is not generally known, and Eq. (4) can only be integrated approximately to give

$$\frac{d\sigma}{d\omega} \approx \frac{2\pi e^4}{mv^2} \frac{1}{E} \left. \frac{df}{d\omega} \right|_{q=q_{\min}} \ln \left[\frac{4E_0}{cE} \right], \quad (5)$$

where q_{\min} is the minimum momentum transfer ($=E/v$) for energy loss E , $E_0 = \frac{1}{2}mv^2$ and c is a constant that depends on the q variation of $df/d\omega$.¹⁰ Bethe⁸ has expressed the total cross section per atom or molecule for ionization of the nl shell (containing Z_{nl} electrons) in the form

$$\sigma = \frac{2\pi e^4}{mv^2} \frac{Z_{nl} b_{nl}}{E_{nl}} \ln \left[\frac{4E_0}{B_{nl}} \right], \quad (6)$$

where B_{nl} is of the order of E_{nl} . Comparing Eqs. (5) and (6),

$$b_{nl} = \frac{ZE_{nl}}{Z_{nl} \ln(4E_0/B_{nl})} \int_{E_{nl}}^{E_{\max}} \frac{1}{E} \left. \frac{df}{d(\hbar\omega)} \right|_{q=q_{\min}} \ln \left[\frac{4E_0}{cE} \right] d(\hbar\omega) \\ \approx \frac{ZE_{nl}}{Z_{nl}} \int_{E_{nl}}^{E_{\max}} \frac{1}{E} \left. \frac{df}{dE} \right|_{q=q} dE, \quad (7)$$

where E_{\max} is large compared to E_{nl} but less than the binding energy of the next most tightly bound shell.

Measurements of energy-loss distributions at zero scattering angle can be used to obtain $(df/d\omega)_{q=q_{\min}}$. For large frequencies ($\hbar\omega \gtrsim 100$ eV) and as $q \rightarrow 0$,

$$-\text{Im}[1/\epsilon(\omega, 0)] \approx \text{Im}[\epsilon(\omega, 0)]$$

⁹ U. Fano, *Ann. Rev. Nucl. Sci.* **13**, 1 (1963).

¹⁰ For atoms, the integration of Eq. (4) has been performed so that $d\sigma/d\omega$ is proportional to the optical oscillator strength $(df/d\omega)_{q=0}$ [see W. F. Miller and R. L. Platzman, *Proc. Phys. Soc. (London)* **70A**, 299 (1957); L. Vriens, *Physica* **31**, 385 (1965)]. In the present work, the electron oscillator strength $(df/d\omega)_{q=q_{\min}}$ depends on the primary electron velocity v . The constant c in the logarithmic factor of Eq. (5) has been assumed here to be unity, in analogy with formulas published by Bethe (Ref. 8) for atomic excitation and ionization, though recent calculations for atomic hydrogen [L. Vriens (private communication)] show that c can depart appreciably from unity for energy losses appreciably greater than the threshold E_{nl} .

to better than 5%.¹¹ With this approximation and the assumption that the "transverse" dielectric constant (determining the optical absorption spectrum) is equal to the "longitudinal" dielectric constant (determining the electron energy-loss spectrum),¹² it is possible to derive x-ray linear absorption coefficients μ_l or mass absorption coefficients μ_m from values of $df/d\omega$ obtained from electron energy-loss measurements. Specifically,

$$\mu_l = \frac{2\pi^2 N e^2}{mc} \left. \frac{df}{d\omega} \right|_{q=q_{\min}} \quad (8)$$

and $\mu_m = \mu_l/\rho$, where ρ is the density of the solid.

3. EXPERIMENTAL PROCEDURE

A. Apparatus

The electron energy-loss spectra were measured in transmission through thin-film specimens at zero scattering angle, using an energy analyzer with a resolution of about 1 eV.^{6,13} The primary beam energy ranged from 20 to 23 keV, depending on the specimen used, and was set to give the optimum beam intensity. The angular acceptance of the analyzer is a cone of half-angle ≈ 0.25 mrad. The angular distribution of the primary beam could be measured by rotating the gun and specimen jointly with respect to the analyzer and was approximately Gaussian with a full angular width at half-maximum of typically 1.6 mrad.

The energy-loss spectra were recorded on an X-Y recorder, plotting electron intensity versus energy loss. A battery in series with the high-voltage lead to the energy analyzer could be switched in to displace the energy-loss spectrum a known amount on the energy-loss scale. Thus a selected portion of the energy-loss spectrum could be recorded while maintaining the absolute energy-loss calibration.

B. Specimen Preparation

The Al specimens were prepared by vacuum evaporation onto a Victawet 35B substrate at a pressure $\approx 10^{-5}$ Torr. The specimens were floated off the substrate on water, and mounted over the 0.5-mm-diam aperture of the specimen holder. The specimen thickness was monitored during the evaporation by a quartz-crystal microbalance. The mass thickness of the specimens used were 8.2 and 5.7 $\mu\text{g}/\text{cm}^2$, which, assuming bulk density,

¹¹ Data for Al over a wide frequency range are presented by H. R. Philipp and H. Ehrenreich, *J. Appl. Phys.* **35**, 1416 (1964). Their values of ϵ near 100 eV were derived from the data of Ref. 5 and show that $-\text{Im}[1/\epsilon(\omega, 0)]$ equals $\text{Im}[\epsilon(\omega, 0)]$ to better than about 5% for $\hbar\omega > 72$ eV. More recent work (see Fig. 4) indicates absorption coefficients several times larger, and hence the difference between $-\text{Im}[1/\epsilon(\omega, 0)]$ and $\text{Im}[\epsilon(\omega, 0)]$ should be smaller than 5%.

¹² V. Ambegaokar and W. Kohn, *Phys. Rev.* **117**, 423 (1960); P. Nozieres and D. Pines, *ibid.* **113**, 1254 (1959).

¹³ L. Marton and J. A. Simpson, *Rev. Sci. Instr.* **29**, 567 (1958).

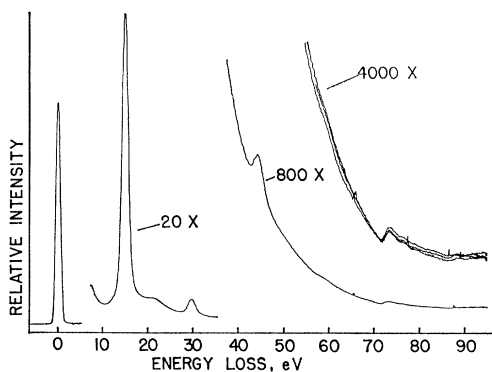


FIG. 1. Energy-loss spectrum of an $8.2\text{-}\mu\text{g}/\text{cm}^2$ -thick Al film. The relative-gain setting is indicated for each intensity change of scale. The zero current level at all gain settings corresponds to the horizontal part of the trace to the left of the elastic peak. The strong loss peak at ≈ 15 eV is due to plasmon excitation, with weaker multiple losses visible at about 30, 45, and 60 eV superimposed on a rapidly decreasing background. Note the size of the step at ≈ 72 eV due to the L_{23} absorption edge compared to the fourth multiple-loss-peak intensity at 60 eV.

correspond to thicknesses of 300 and 210 Å. The uncertainty in these film thicknesses is 5–10%.

Al_2O_3 films were prepared in two ways. Several 300 Å-thick Al films were mounted on Pt specimen holders and heated in air to about 700°C for 7 h, producing transparent, continuous films of $\gamma\text{-Al}_2\text{O}_3$ over the apertures.¹⁴ If oxidation were complete, these films would be $15.5\ \mu\text{g}/\text{cm}^2$ thick. Anodized amorphous Al_2O_3 films were prepared in several thicknesses ranging from 410 to 575 Å,¹⁵ and were mounted on the specimen holders by floating small sections on water. A mass thickness was determined by weighing a known film area on a sensitive microbalance, with an uncertainty of about 10%. The density of these films was $2.8\ \text{g}/\text{cm}^3$, using the film thicknesses calculated from the anodization procedure. An investigation of the 0–40-eV energy-loss region¹⁶ for each form of Al_2O_3 indicates essentially complete oxidation.

C. Treatment of the Data

Figure 1 shows an energy-loss spectrum for a 300 Å-thick Al film with the appropriate intensity scale factors indicated. The 15-eV characteristic energy-loss peak due to plasmon excitation is the dominant feature, with the multiple losses at 30, 45, and 60 eV successively diminishing in intensity. At about 72 eV there is an increase in energy-loss intensity associated with the excitation of the L -shell electrons. It should be emphasized that Fig. 1 does not represent a measure of the differential cross section for zero scattering angle as a function of energy loss. The angular resolution of the apparatus was comparable with the half-width of the

inelastic angular distribution (a function of energy loss E) and the system would detect more electrons of low E than of high E for two loss processes of identical cross section. It was therefore necessary to use thin specimens so that multiple plasmon-loss peaks did not obscure the features of interest; the films had to be thick enough, however, to be self-supporting and to eliminate angle-dependent corrections due to surface effects.¹⁷

Figure 2(a) shows the energy-loss region from 70 to 130 eV for the same Al specimen. From both Figs. 1 and 2 it is apparent that the energy-loss intensity from the excitation of the L -shell electrons is superimposed on the decreasing tail of the characteristic (valence-electron) loss spectrum. A reliable estimate of this "background" must be made in order to measure the intensities corresponding to the inner-shell excitation (ISE) as required for the calculation of oscillator strengths and cross sections. The choice of background also determines the positions of the observed structure.

It was initially thought that the background was due entirely to the overlapping tails of the multiple plasmon

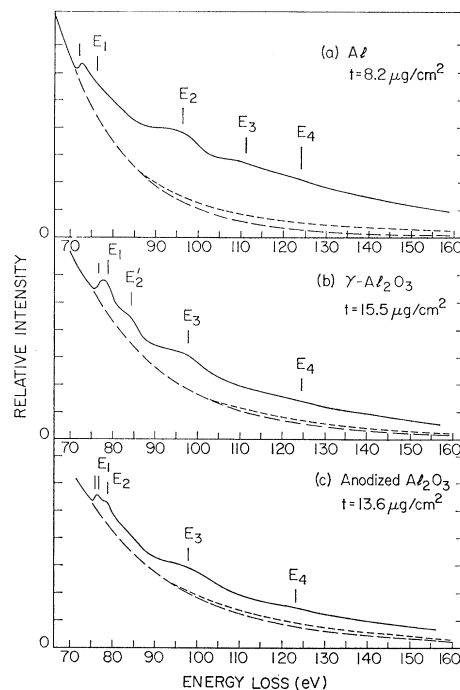


FIG. 2. Energy-loss spectra in the energy region corresponding to L -shell excitation. (a) Al. (b) $\gamma\text{-Al}_2\text{O}_3$ prepared by oxidizing an Al film in air. (c) Anodized Al_2O_3 . Film thicknesses are indicated for each specimen. The positions of absorption edges and loss-spectra maxima are marked by vertical lines (see Tables I and II). The backgrounds calculated by extrapolation of the energy-loss intensities below the absorption edges are shown as long-dashed lines (see Sec. 3C); the additional contributions to the loss intensities from electrons exciting both a plasmon and an inner-shell electron are shown as short-dashed lines. The measured intensity of inner-shell excitation processes in each loss spectrum was that above this combined background.

¹⁴ G. Hass, *Z. Anorg. Chem.* **254**, 96 (1947). $\gamma\text{-Al}_2\text{O}_3$ densities are typically $3.5\text{--}3.9\ \text{g}/\text{cm}^3$.

¹⁵ H. Johnson and R. D. Deslattes, *Rev. Sci. Instr.* **36**, 1381 (1965).

¹⁶ N. Swanson, *Phys. Rev.* **165**, 1067 (1968).

¹⁷ P. Schmüser, *Z. Physik* **180**, 105 (1964).

peaks. On this basis, it would have been possible to synthesize a loss spectrum, based on the line shape for the 15-eV plasmon loss, and to use this computed spectrum to predict the background in the ISE region. The frequency-dependent dielectric constant can be approximately expressed in the Drude form¹⁸:

$$\epsilon(\omega) = 1 - \omega_p^2 / \omega(\omega + i\gamma), \quad (9)$$

where $\omega_p = (4\pi n e^2 / m)^{1/2}$, n is the valence-electron density, and γ is a characteristic damping frequency. The contribution of interband transitions to $\epsilon(\omega)$ has been neglected, and it is not possible to use Eq. (9) to predict accurately the position and intensity of a plasmon energy loss in Al. One can, however, use the Drude form for $\epsilon(\omega)$ to describe the line shape of a volume plasmon loss by the function¹⁹

$$-\text{Im} \left[\frac{1}{\epsilon(\omega)} \right] = \frac{\omega \gamma_v \omega_v^2}{(\omega^2 - \omega_v^2)^2 + \omega^2 \gamma_v^2}, \quad (10)$$

where the frequency ω_v is derived from the experimental loss position $\hbar\omega_v$ and γ_v from the observed half-width $\hbar\gamma_v$. It is similarly possible to describe the line shape of a surface plasmon-loss peak²⁰ where the metal surface is covered with an oxide layer of dielectric constant ϵ_B by the function

$$-\text{Im} \left[\frac{1}{\epsilon(\omega) + \epsilon_B} \right] = \frac{\omega \gamma_s \omega_s^4}{\omega_s^2 [(\omega^2 - \omega_s^2)^2 + \omega^2 \gamma_s^2]}, \quad (11)$$

where again the experimental parameters ω_s and γ_s describing the surface loss are used.

Starting with a primary no-loss beam assumed to have a Gaussian line shape, characteristic loss spectra have been computed by successive folding calculations using Eqs. (10) and (11) in which the intensities of the various peaks have been normalized to correspond approximately with those observed. The results of such a calculation for Al are shown in Fig. 3, where the surface plasmon loss has been included by folding with the primary beam and the first three multiples of the volume plasmon loss. The parameters used in this calculation were $\hbar\omega_v = 14.8$ eV, $\hbar\gamma_v = 0.9$ eV, $\hbar\omega_s = 6.8$ eV, $\hbar\gamma_s = 1.6$ eV, and the half-width of the primary beam = 1.75 eV.²¹

It was found that no reasonable adjustment of the parameters could give a useful representation of the observed spectrum, there being approximately

¹⁸ N. F. Mott and H. Jones, *The Theory of the Properties of Metals and Alloys* (Clarendon Press, Oxford, England, 1936), p. 112.

¹⁹ N. Swanson, *J. Opt. Soc. Am.* **54**, 1130 (1964).

²⁰ R. H. Ritchie, *Phys. Rev.* **106**, 874 (1957); E. A. Stern and R. A. Ferrell, *ibid.* **120**, 130 (1960).

²¹ J. Geiger and K. Wittmaack, *Z. Physik* **195**, 44 (1966) found $\hbar\gamma_v = 0.60$ eV using a monochromatized electron beam and high-resolution energy analyzer. There is evidence [C. von Festenberg, *Phys. Letters* **23**, 293 (1966)] that the loss half-width depends on crystallite size, and $\hbar\gamma_v = 0.9$ eV is more representative of the Al films produced in this laboratory.

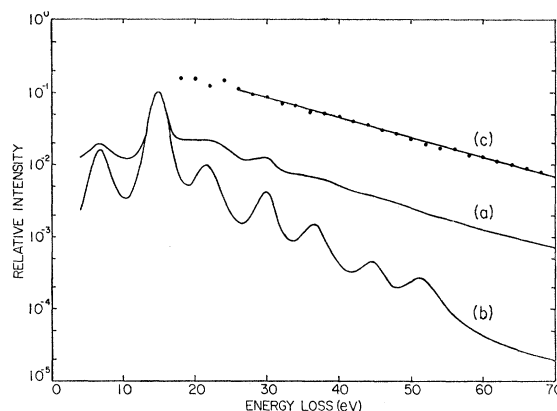


FIG. 3. Plot on a logarithmic scale of characteristic loss spectra of Al. Curve (a) is the observed spectrum (210 Å specimen), and curve (b) is the spectrum computed using the folding procedure discussed in Sec. 3C. Curve (c) is a plot of 10× the difference between curves (a) and (b); relatively large surface-plasmon-loss contributions were included in (b) to make plot (c) approximately linear.

an order of magnitude difference in the intensities at $E = 70$ eV energy loss if the curves were normalized to coincide at $E = 14.8$ eV. It was realized that the difference between the experimental and computed spectra was due to such factors as the occurrence of interband transitions in Al,^{5,22} to inelastic scattering in the oxide layers on the specimen surfaces, to the inadequacy of Eqs. (9)–(11), and to the variation of effective angular resolution with E . The background in the ISE region was therefore regarded as being of two parts: a contribution due to plasmon peaks which could be estimated by the folding calculation, and a contribution due to the approximations and omissions just described. The latter portion, the difference between the observed and computed spectra, is shown in Fig. 3 and could be fitted by least squares with a decreasing exponential function. This function could be extrapolated into the ISE region, and a total background found by adding the plasmon contribution from the folding calculation. The exponential function was one of several functions used in trial fits and yielded the least imprecision in the region of extrapolation; there is however, no *a priori* justification for the use of such a function. It is difficult to estimate the magnitude of any systematic error on this account because no independent data of sufficient reliability exist to estimate the magnitude of all the effects contributing to the difference between the observed and computed spectra in Fig. 3.

Similar background calculations have been made for the two forms of Al_2O_3 ; in each case, it was only necessary to consider the ≈ 23 -eV loss¹⁶ and one multiple of this loss. The scatter in the data points [as in Fig. 3(c)] was such that the uncertainty in the extrapolated intensity for the largest energy loss considered was less

²² H. Ehrenreich, H. R. Philipp, and B. Segall, *Phys. Rev.* **132**, 1918 (1963).

TABLE I. Positions of the absorption edge and maxima in the energy-loss spectrum of Al, as marked in Fig. 2(a). The number of measurements on each structure is given under n . The stated errors are the standard deviation of a single measurement, for seven or more measurements, and are estimates, for less than seven measurements. The positions of structure in Watanabe's (Ref. 4) energy-loss measurements, in the μ_m derived here (Fig. 4), and in two soft-x-ray absorption measurements (Refs. 23 and 24) are also shown. All energies are in eV.

Structure	n	Electron energy loss		x-ray absorption		
		Present work	Watanabe	Derived from present work	Codling and Madden	Fomichev and Lukirskii
L_{23} edge	13	72.5 ± 0.5	72		72.72^a	≈ 72
E_1	3	76.3 ± 1^b		76.8		76
			82		84 (weak)	84 (weak)
E_2	9	96.3 ± 0.5	94	96.8	96	96
E_3	6	111.2 ± 1		111.7	~ 117	112
E_4	6	124.2 ± 1		124.7		125

^a L_3 edge.

^b Possibly due to Al_2O_3 .

than 2%, except for the γ - Al_2O_3 , where it was less than 7%.

Another correction to the observed intensity in the ISE region is the contribution from electrons which have undergone one (or more) valence-electron characteristic loss processes in addition to having excited an inner-shell electron. Since Poisson statistics hold for inelastic-scattering processes, it can be shown that for sufficiently thin films and at zero scattering angle, the ratio of the number of electrons undergoing one characteristic loss process and an ISE process to the number of electrons undergoing only an ISE process is very nearly equal to the ratio of the first characteristic-loss-peak area to the elastic (no loss) peak area. We can neglect the probability of two characteristic loss events and an ISE compared to the probability of an ISE alone, at zero scattering angle. This additional background correction is shown in Fig. 2 as a short-dashed line.

The intensities and positions of the structure observed in the various ISE spectra were measured assuming the combined background discussed above. Differential oscillator strengths, x-ray-absorption coefficients, and total electron-scattering cross sections for inner-shell excitation were calculated from these intensities using a comparison technique described in Sec. 5.1 of Ref. 6. The technique consists of folding the primary-beam angular distribution with the differential cross section to correct the zero-angle spectrum for finite angular resolution and to determine the fraction of the angular distribution not measured. A specimen with an energy-loss process of known cross section is used as a comparison standard to minimize the effects of uncertainties in the angular characteristics of the apparatus; in this work, ISE intensities were compared with the 14.8 energy-loss intensity in Al.⁶

4. RESULTS

A. Energy-Loss Peaks and Comparison with x-Ray-Absorption Data

The locations of prominent structure in the energy-loss spectra were measured, as illustrated in Fig. 2.

The absorption edge was taken to lie midway between the top and the bottom of the step occurring at the onset of ISE, because of the ≈ 1 eV full width at half-maximum (FWHM) energy spread of the primary electron beam. (In principle, the absorption edge should lie at the point of inflection of the initial rise in energy-loss intensity, but in practice this point could never be clearly distinguished.) The L_2 and L_3 edges could not be resolved for any of the specimens, and are referred to jointly as the L_{23} edge.

The number of measurements of any given loss peak or absorption edge varied from as few as three up to 21. The mean of the energy-loss values was used in each case. If seven or more measurements were made, the standard deviation of a single measurement was computed. If less than seven measurements were made, the estimated uncertainty in the measurement was used for the error. The confidence coefficient is 0.95 that the mean of seven measurements is within one standard deviation of the true value, in the absence of systematic error. In all cases of seven or more measurements, the values appeared to be randomly distributed about the mean. Measurements were made with three Al specimens (two of 300 Å and one of 210 Å thickness), three anodized Al_2O_3 (of 410, 480, and 575 Å thickness) and two γ - Al_2O_3 films.

The results for Al are shown in Table I. For comparison, the results of Watanabe⁴ obtained from electron energy-loss measurements at 50 keV, the measurements by Codling and Madden²³ for the soft-x-ray absorption spectrum of Al using the continuum radiation from the NBS synchrotron, and the results of Fomichev and Lukirskii²⁴ for x-ray absorption using bremsstrahlung are also shown. A group²⁵ using the Tokyo University synchrotron has obtained similar results in the 70–100-eV region.

²³ K. Codling and R. P. Madden, preceding paper, Phys. Rev. **167**, 587 (1968).

²⁴ V. A. Fomichev and A. P. Lukirskii, Fiz. Tverd. Tela **8**, 2104 (1966) [English transl.: Soviet Phys.—Solid State **8**, 1674 (1967)]; V. A. Fomichev, *ibid.* **8**, 2892 (1966) [English transl.: *ibid.* **8**, 2312 (1967)].

²⁵ T. Sagawa, Y. Iguchi, M. Sasanuma, A. Ejiri, S. Fujiwara, M. Yokota, S. Yamaguchi, M. Nakamura, T. Sasaki, and T. Oshio, J. Phys. Soc. Japan **21**, 2602 (1966).

TABLE II. Positions of the absorption edge and maxima in the energy-loss spectra of Al_2O_3 prepared by anodization and by oxidizing Al films in air ($\gamma\text{-Al}_2\text{O}_3$), as marked in Figs. 2(b) and 2(c). The number of measurements on each structure is given under n . The stated errors are the standard deviation of a single measurement, for seven or more measurements, and are estimates, for less than seven measurements. For comparison, the positions of corresponding structure in Watanabe's energy-loss measurements (Ref. 4) and the soft-x-ray absorption measurements of Codling and Madden (Ref. 23) and of Fomichev (Ref. 24) are shown. The peaks in μ_m (Fig. 4) derived from Figs. 2(b) and 2(c) occur about 0.5 eV above the stated energy-loss values. All energies are in eV.

Structure	n	Electron energy loss			x-ray absorption		
		Present work		Watanabe Anodized Al_2O_3	Codling and Madden		Fomichev Anodized Al_2O_3
		Anodized Al_2O_3	n		$\gamma\text{-Al}_2\text{O}_3$	Anodized Al_2O_3	
L_{23} edge	21	75.8 ± 0.5	9	76.9 ± 0.4	76.48	77.41	76.3
E_1	17	76.7 ± 0.6	7	78.8 ± 0.4	77	77.1	76.8
						78.6 (weak)	
E_2	20	79.0 ± 0.5			79	79.8	79.5
E_2'			7	83.9 ± 0.4		86	84.5
E_3	10	97.8 ± 0.7	7	98.2 ± 0.5	94	99	98
							110
E_4	5	123.3 ± 1.5	4	124.2 ± 1.5			124

The Al L_1 edge has been reported to lie at 117.7 ± 0.4 eV,²⁶ but no peak could be seen near this energy on any of the loss spectra. This is not surprising, because the L_1 hole is short-lived and it is also possible that the L_1 oscillator strength is distributed over a relatively large energy range. Watanabe^{4,25} has attributed the peak at 111 eV to the combination of a ≈ 96 -eV loss process and a 15-eV plasmon loss. However, the present results still show a weak peak at ≈ 111 eV after the characteristic loss contribution is subtracted. The weak loss at 76.3 eV may be due to the surface layer of Al_2O_3 . This layer is amorphous in character,¹⁴ and the loss position corresponds to that found for the L_{23} edge of anodized Al_2O_3 .

The anodized Al_2O_3 and the $\gamma\text{-Al}_2\text{O}_3$ prepared by oxidizing Al films in air gave slightly different energy-loss spectra, corresponding to differences in the two materials first noticed by Codling and Madden²³ in their soft-x-ray absorption measurements. The L_{23} absorption edges are several eV higher in energy than the Al L_{23} edge, and appear to be about 1 eV apart. The anodized (amorphous) film has a clearly resolved doublet peak at about 77 and 79 eV, while the polycrystalline film has only one pronounced peak near the absorption edge, which, from Codling and Madden's data at higher resolution, would appear to be several closely spaced narrow peaks not resolved here. Fomichev²⁴ has also measured the soft-x-ray absorption spectrum of anodized Al_2O_3 and his results agree well with those found here. The measured positions of the absorption edge and the energy-loss peaks are listed in Table II, together with the energy-loss measurements of Watanabe for anodized films, and the soft-x-ray measurements of Codling and Madden and of Fomichev.

B. Oscillator Strengths, Absorption Coefficients, and Cross Sections

ISE spectra were recorded 40–90 eV beyond the absorption edge for each of the specimens. Three of the

best loss spectra were selected in each case for obtaining differential oscillator strengths, total cross sections, absorption coefficients, and values of $n_{\text{eff}}(E)$ using the appropriate equations of Sec. 2 [and assuming $c=1$ in Eq. (5)].

The results for a 300 Å-thick Al film are given in Figs. 4 and 5 and Table III for a primary energy of 21 keV. The results of the three ISE spectra agreed to about 30%; the reason for this large imprecision is not clear, though it might be due to changes in the degree of axial symmetry of the gun-analyzer system from run to run. The results based on three ISE spectra of each of the Al_2O_3 specimens at 21 keV are also shown in Figs. 4 and 5 and Table III. These results agreed to about 10% for each kind of Al_2O_3 .

The uncertainties in the calculated values of σ , $df/d\omega$, and μ_m arise from the 25% uncertainty in the cross section of the Al 14.8-eV loss used as a standard,⁶ together with the uncertainties in the various experimental quantities involved in the comparison technique. Combining the uncertainty in the standard cross section quadratically with the estimated errors in the comparison technique leads to an estimated error of about

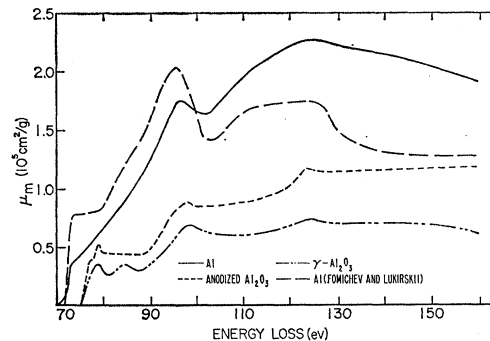


FIG. 4. Results for the mass absorption coefficient μ_m from the ISE measurements on Al and Al_2O_3 . For comparison, the Al data of Fomichev and Lukirskii are included; the precision in their determinations of μx (x is the specimen thickness) was about $\pm 5\%$ and to derive μ_m it has been assumed that their films were of bulk density and that there was negligible error in their stated x .

²⁶ A. Fahlman, K. Hamrin, R. Nordberg, C. Nordling, and K. Siegbahn, Phys. Rev. Letters 14, 127 (1965).

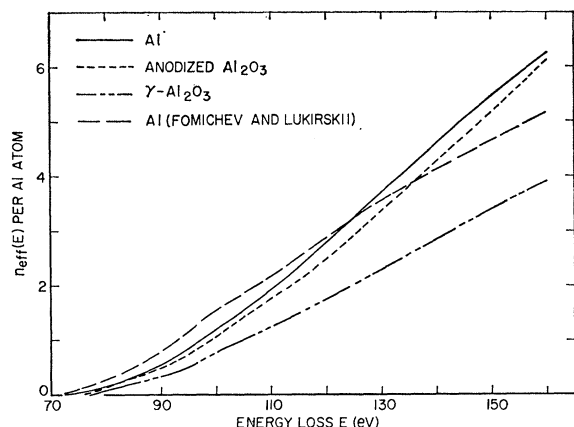


FIG. 5. The effective number of electrons per Al atom participating in inner-shell excitation processes versus energy loss obtained from the energy-loss measurements on Al and Al_2O_3 . For comparison, values of $n_{\text{eff}}(E)$ were calculated using Eqs. (8) and (3b) from the $\mu_i(E)$ data for Al measured by Fomichev and Lukirskii (Fig. 4).

40% in the results for σ , $df/d\omega$, and μ_m for the three materials.

5. DISCUSSION

A. Positions of the ISE Structure

The positions of the structure in the ISE spectra for the three materials in general agree very well with measurements of x-ray absorption using continuous x-radiation sources. A few weak peaks seen in x-ray absorption are not detected or resolved in the ISE spectra.

The chemical shift of the L_{23} edge from Al metal to the oxide in the ISE measurements was 3.3 eV for anodized Al_2O_3 and 4.4 eV for $\gamma\text{-Al}_2\text{O}_3$. Codling and Madden's results for this shift are somewhat larger, 4.0 and 4.9 eV, respectively,²³ although the differences in the results for each material are within the experimental uncertainty. In K -absorption measurements, Rudström²⁷ found a chemical shift of the K -absorption edge

TABLE III. Cross-section parameters for L -shell excitation in Al and Al_2O_3 for 21-keV primary electron energy. Cross sections (per atom or molecule) and values of $n_{\text{eff}}(160)$ [Eq. (3b)] and b_{nl} [Eq. (7)] were obtained from the experimental distributions of oscillator strength. The b_{nl} values were determined for all L -shell electrons using the average Al L -shell binding energies E_{nl} indicated. As there are two Al atoms per Al_2O_3 molecule, the Al_2O_3 parameters are expressed to indicate the values per Al atom. The estimated error of each quantity is discussed in Sec. 4B.

	Al	Anodized Al_2O_3	$\gamma\text{-Al}_2\text{O}_3$
Range of integration (eV)	72–160	75–160	76–160
Cross section per atom or molecule (10^{-18} cm ²)	1.08	2×1.03	2×0.67
$n_{\text{eff}}(160)$	6.3	2×6.1	2×3.9
b_{nl}	0.55	0.55	0.36
E_{nl} (eV)	83	87	87

²⁷ L. Rudström, Arkiv Fysik 12, 287 (1957).

of 5.3 eV for anodized Al_2O_3 compared to Al. Deslattes²⁸ in a similar measurement found a shift of 5.8 eV. Due to the possibility of different K - and L -shell binding energies in the Al and Al_2O_3 , however, a direct comparison with the L_{23} absorption-edge shift is not significant. For similar reasons, a direct connection between the Al_2O_3 band gap and the chemical shift of the L_{23} edge cannot be made.

A complete theory to describe the positions and intensity of the fine-structure maxima observed on the high-energy side of x-ray absorption edges does not exist.²⁹ A number of authors,³⁰ however, have measured the effects of crystalline structure on the absorption fine structure and have compared the fine structure of an element and a number of its compounds. In most cases, crystalline and noncrystalline phases of a material may show similar though not necessarily identical fine-structure spectra. The fine structure in different oxides of some transition metals has been shown by White and McKinstry³⁰ to be dependent on the bond character and the nearest-neighbor environment. The crystalline and amorphous forms of Al_2O_3 show similar fine structure (Fig. 2), except for the region close to the absorption edge, where x-ray absorption measurements²³ show more structure in the crystalline than in the amorphous phase. In addition, the fine-structure spectra of both oxides is qualitatively similar to the fine structure of Al (Fig. 4), though this similarity is probably fortuitous.

B. Absorption Coefficients

Few measurements have been made of absorption coefficients in the ultrasoft x-ray region. Tomboulou and Pell⁵ measured μ_i for Al films both self-supporting and on a Zapon substrate, obtaining results which differed by roughly a factor of 3 for the two cases. A recent measurement by Fomichev and Lukirskii²⁴ using bremsstrahlung incident on ≈ 1000 Å-thick Al films, both self-supported and on a nitrocellulose base, gave values of μ_i larger than Tomboulou and Pell's results and comparable to those found here.

Henke *et al.*³¹ derived semiempirical values of μ_m for various elements in the 5–50 Å (2500–250 eV) region. If we extend Henke's "universal absorption" function to lower energy, we obtain for Al $\mu_m \approx 9.0 \times 10^4$ cm²/g

²⁸ R. D. Deslattes (private communication).

²⁹ L. V. Azaroff, Rev. Mod. Phys. 35, 1012 (1963).

³⁰ W. F. Nelson, I. Siegel, and R. W. Wagner, Phys. Rev. 127, 2025 (1962); W. M. Weber, Physica 30, 2219 (1964); E. Alexander, S. Feller, B. S. Fraenkel, and J. Perel, Nuovo Cimento 35, 311 (1965); F. W. Lytle, in *Proceedings of the International Conference on the Physics of Non-Crystalline Solids, Delft, 1964*, edited by J. A. Prins (North-Holland Publishing Co., Amsterdam, 1965), p. 12; E. W. White and H. A. McKinstry, Advan. X-Ray Anal. 9, 376 (1965); A. Meisel, Phys. Status Solidi 10, 365 (1965); J. Perel, Phys. Rev. 147, 463 (1966); O. Brümmer and G. Dräger, Phys. Status Solidi 14, K175 (1966).

³¹ B. L. Henke, R. White, and D. Lundberg, J. Appl. Phys. 28, 98 (1957).

at 155 eV. Recent measurements³² of μ_m for Al are 25–30% larger than the values predicted by Henke for $850 < E < 1000$ eV, the difference increasing as the energy decreases. We might infer, then, that the value obtained from Henke's functions at 155 eV is at least 30% low, or that $\mu_m(155 \text{ eV}) \geq 1.2 \times 10^5 \text{ cm}^2/\text{g}$. A new x-ray measurement at 278 eV by Singer³³ has led to a similar conclusion.

The Al absorption-coefficient measurements of Fomichev and Lukirskii have been plotted in Fig. 4 assuming bulk density, together with the values of μ_m derived from the ISE spectra. The results are in reasonably good agreement and consistent with the lower bound estimated using Henke's function and Bearden's data, while Tombouliau's⁵ values for μ_m are considerably smaller. Fomichev's²⁴ absorption coefficients for anodized Al_2O_3 are also in good agreement with those found here. The experimental errors in the absolute determinations of μ_m , however, are such that absorption coefficients for $\gamma\text{-Al}_2\text{O}_3$ (for $\hbar\omega > 90$ eV) are not believed to be significantly different from those of anodized Al_2O_3 . The ratio of μ_m for each oxide to that for Al is comparable to the proportion by weight of Al in each material.

C. Ionization Cross Sections

Cross sections for ionization of particular shells in several solids have previously been obtained by measuring the resultant x-ray yields.³⁴ These results can be used to derive values of the two constants b_{nl} and B_{nl} in Eq. (6), applicable to all atoms, or can be compared in a few cases with more detailed calculations for specific atoms.³⁵ Though Bethe⁸ has tabulated values of b_{nl} for a number of atoms and for various values of n and l , these estimates do not take account of transitions forbidden by occupation of the inner shells. While Eq. (3a) represents a sum rule on $df/d\omega$ for all electronic excitations, a partial-sum rule does not exist; that is, an integration of $df/d\omega$ over an energy region corresponding to excitations of the nl shell does not yield a value of $n_{\text{eff}}(E \rightarrow E_{\text{max}})$ equal to Z_{nl} .³⁶ Thus b_{nl} cannot be derived from theory without calculation of $df/d\omega$ for each atom. It would, however, be expected [Eq. (7)] that b_{nl} would be of order unity.

³² B. A. Cooke, K. A. Pounds, P. C. Russell, and E. A. Stewardson, Proc. Phys. Soc. (London) **79**, 883 (1962); A. J. Bearden, J. Appl. Phys. **37**, 1681 (1966).

³³ S. Singer, J. Appl. Phys. **38**, 2897 (1967).

³⁴ J. C. Clark, Phys. Rev. **48**, 30 (1935); A. E. Smick and P. Kirkpatrick, *ibid.* **67**, 153 (1945); M. Green and V. E. Cosslett, Proc. Phys. Soc. (London) **78**, 1206 (1961); M. Green, in *X-Ray Optics and X-Ray Microanalysis*, edited by H. H. Pattee, V. E. Cosslett, and A. Engström (Academic Press Inc., New York, 1963), p. 185; A. J. Campbell, Proc. Roy. Soc. (London) **A274**, 319 (1963); J. W. Motz and R. C. Placiou, Phys. Rev. **136**, A662 (1964); W. Hink, Z. Physik **177**, 424 (1964); **182**, 227 (1965).

³⁵ A. M. Arthurs and B. L. Moiseiwitsch, Proc. Roy. Soc. (London) **A247**, 550 (1958); H. S. Perlman, Proc. Phys. Soc. (London) **76**, 623 (1960).

³⁶ A. H. Compton and S. K. Allison, *X-Rays in Theory and Experiment* (D. Van Nostrand and Co., Inc., New York, 1935).

X-ray-yield measurements³⁴ indicate values of b_{nl} between about 0.5 and 1.5. Values of b_{nl} derived from the present work are shown in Table III; due to the small range of energy integration, these values would be low by about 50%. The ionization cross sections for the same energy-loss region are also shown in Table III; these cross sections would probably be at least 50% larger if oscillator-strength contributions over a wider and more realistic energy-loss region could be measured (with the necessary precision) and included.

X-ray absorption measurements on alloys and compounds^{30,37} show that $df/d\omega$ generally changes from the distributions characteristic of the parent elements. The possibility of resultant change in b_{nl} could be important in high-precision quantitative electron-probe microanalysis; hitherto, it has been implicitly assumed that atomic b_{nl} values did not change with compounding or alloying.

D. Oscillator-Strength Sum Rule

The values of $df/d\omega$ derived from the ISE spectra have been used to derive the effective number of L-shell electrons per Al atom contributing to the observed absorption [Eq. (3b)]. Figure 5 shows plots of $n_{\text{eff}}(E)$ per Al atom for Al and the two forms of Al_2O_3 , as well as a plot of $n_{\text{eff}}(E)$ derived from the values of μ_l for Al measured by Fomichev and Lukirskii.²⁴

It is convenient to break the integration [Eq. (3a)] into three regions when considering Al or Al_2O_3 , and to define

$$\bar{n}_K = Z \int_{E_K}^{\infty} \frac{df}{dE} dE, \quad (12a)$$

$$\bar{n}_L = Z \int_{E_L}^{E_K} \frac{df}{dE} dE, \quad (12b)$$

$$\bar{n}_{\text{val}} = Z \int_0^{E_L} \frac{df}{dE} dE, \quad (12c)$$

where \bar{n}_K , \bar{n}_L , and \bar{n}_{val} represent the number of Al electrons per atom (or molecule in Al_2O_3) contributing to df/dE in the three energy regions which are delineated by the Al K- and L_{23} -shell binding energies. For Al, \bar{n}_{val} is approximately three^{6,11} and \bar{n}_K is between 1.4 and 2.0.¹¹ Therefore, \bar{n}_L should be between 8 and 9.

For photon energies between about 200 and 10^4 eV, df/dE has been empirically found to vary as E^{-a} (away from absorption-edge regions), where a is between 2.7 and 3.^{31,36} While the values of df/dE derived here are not varying as E^{-a} in the region of measurement, df/dE has been arbitrarily assumed to vary as E^{-3} for $E > 160$ eV, from which \bar{n}_L has been found to be 12.2, about twice the value of $n_{\text{eff}}(160)$ shown in Table III,

³⁷ B. N. Das and L. V. Azaroff, Acta Met. **13**, 827 (1965).

which was obtained by integration from 72 to 160 eV (Fig. 4). Considering the accuracy of the present determinations of df/dE and the arbitrary nature of the extrapolation, the value of \bar{n}_L is in reasonable agreement with the value expected. The apparent discrepancy in the sum-rule evaluation of Philipp and Ehrenreich,¹¹ based on early absorption data,⁵ is therefore removed with the present results and the recent soft-x-ray absorption measurements.²⁴

Again using an E^{-3} extrapolation, values of \bar{n}_L of 2×13.0 and 2×7.5 have been found for anodized and γ - Al_2O_3 , respectively.³⁸ These values are also about twice the values of $n_{\text{eff}}(160)$ shown in Table III.

6. CONCLUSION

Structure observed in the electron energy-loss spectra corresponding to L -shell excitation in Al and Al_2O_3 is in good agreement with structure observed in soft-x-ray absorption measurements on the same materials. By choosing a reasonable background for the energy-loss spectra and performing a correction for the finite angular resolution of the apparatus, values of oscillator strengths, mass absorption coefficients, and electron-scattering cross sections have been derived for these materials up to about 80 eV beyond the absorption edge. The Al and Al_2O_3 results appear reasonable both from the point of view of self-consistency and when compared with the most recent x-ray measurements of μ_m for Al. These results are consistent with the equality of the longitudinal and transverse dielectric constants and the expectation that in this energy region $\epsilon_1 \approx 1$ and $\epsilon_2 \ll 1$, so that the optical-absorption parameter ϵ_2 is to a good approximation equal to the electron energy-loss function $-\text{Im}\epsilon^{-1}$.

³⁸ The numerical results are shown in this form to take account of the two Al atoms per molecule and to indicate the effective number of electrons per Al atom participating in the absorption.

It has been shown that the cross sections for ionization of inner-shell electrons in solids can be measured more directly than by finding the yield of x rays following the decay of the particular excited state. The accuracy of the cross-section measurements in the present work has not been high, though it is believed that this could be significantly improved by using an apparatus with poorer angular resolution than that used here. Though it might seem from Fig. 1 that the loss intensity due to L -shell excitation is a small fraction of that of the 14.8-eV loss, it has been found here that the total cross section per Al atom for L -shell excitation is about $\frac{1}{4}$ of that for the plasmon loss.⁶ With apparatus better suited to measuring energy losses due to inner-shell excitation in solids, it would be possible to use thicker specimens, eliminate or reduce the uncertainties in the estimation of the background, as discussed in Sec. 3 C, and to make more precise estimates of loss intensity over a more extensive energy-loss range. If a comparison technique like that used here was adopted in similar work, it would be desirable to know the cross section for the standard loss more accurately. In addition, attempts should be made to ascertain more precisely the extent to which crystalline order and orientation affect the inelastic processes of interest.³⁹

ACKNOWLEDGMENTS

We are indebted to Dr. K. Codling for providing us with the results of his soft-x-ray absorption measurements, and to Dr. Codling, Dr. R. P. Madden, Dr. R. E. LaVilla, Dr. R. D. Deslattes, and Dr. H. Mendlowitz for beneficial discussions. We would like to thank Harold Johnson for making the anodized Al_2O_3 films.

³⁹ P. Duncumb, *Phil. Mag.* **7**, 2101 (1962); A. Howie, *Proc. Roy. Soc. (London)* **A271**, 268 (1963); F. Bell and R. Sizmann, *Phys. Letters* **19**, 171 (1965); R. Uyeda and M. Nonoyama, *J. Appl. Phys. Japan* **4**, 498 (1965); C. R. Hall, *Proc. Roy. Soc. (London)* **A295**, 140 (1966).